ADVANCED MATERIALS
www.advmat.de

Stereoselective Synthesis, Efficient Light Emission, and High Bipolar Charge Mobility of Chiasmatic Luminogens

*Zujin Zhao, Jacky W. Y. Lam, Carrie Y. K. Chan, Shuming Chen, Jianzhao Liu, Ping Lu, Mario Rodriguez, José-Luis Maldonado, Gabriel Ramos-Ortiz, Herman H. Y. Sung, Ian D. Williams, Huimin Su, Kam Sing Wong, Yuguang Ma, Hoi Sing Kwok, Huayu Qiu, and Ben Zhong Tang**

Synthesis of fluorophores with novel molecular structures have attracted much attention in the past two decades because such materials may exhibit unique properties that enable them to find an array of applications in optoelectronics and biological science. In previous studies, we found that a series of propeller-like luminogens that were non-fluorescent in solution became strong emitters when aggregated in poor solvents or fabricated as thin films, thus demonstrating a novel phenomenon of aggregation-induced emission (AIE).[1] Systematic studies have rationalized that restriction of intramolecular rotation (IMR) is the main cause for the AIE effect, which blocks the nonradiative relaxation channels and populates the radiative decay.[2] Among the AIE luminogens, tetraphenylethene (TPE) is a prototype molecule. Studies have revealed that the IMR process of TPE can be inhibited by many external factors, such as solvent viscosity, temperature, pressure, etc.[3] However, there are few reports on the internal control on the IMR process at the molecular level.[2a,4] We envision that imparting a highly rigid molecular structure to TPE may hinder its IMR process and thus change the emission behavior of the luminogen accordingly. Herein, we present the synthesis of two TPE derivatives featured with cross-shaped (chiasmatic) molecular conformations and report their photoluminescence (PL), electroluminescence (EL), and charge transport properties.

The chiasmatic luminogens (*Z*)-1,2-bis[4′-(9-carbazolyl) biphenyl-2-yl]-1,2-diphenylethene [(*Z*)-*o*- BCaPTPE] and (*Z*)-1,2-bis[4′-(diphenylamino)biphenyl-2-yl]-1,2-diphenylethene [(*Z*)-*o*-BTPATPE]] were synthesized by McMurry reaction[5] of 2-arylbenzophenones, as illustrated in **Scheme 1**. For comparison, we also prepared their linear counterparts 1,2-bis[4′-(9-carbazolyl)biphenyl-4-yl]-1,2-diphenylethene (*p*-BCaPTPE and 1,2-bis[4′-(diphenylamino)biphenyl-4-yl]-1,2-diphenylethene (*p*-BTPATPE)) under similar experimental conditions. Detailed synthetic procedures, characterization data, and ^{1}H NMR spectra are given in the Supporting Information and Figure S1–S3 (Supporting Information). It is well known that McMurry reaction of unsymmetrical diarylketones generally gives stereorandom products with Z/E ratios of ≈50/50%.[6] In some occasions, the *Z* and *E*-isomers can be separated by column chromatography or recrystallization but the efficiency is normally quite low. On the contrary, we obtained *o*-BCaPTPE and *o*-BTPATPE with solely *Z* stereostructure from their corresponding benzophenones in moderate yields (52% and 59% for (*Z*)-*o*-BCaPTPE and (*Z*)-*o*-BTPATPE, respectively). Their structures were confirmed by single-crystal X-ray diffraction. Their ORTEP (Oak Ridge thermal ellipsoid plot) drawings are shown in **Figure 1**, and the crystal data are provided in Table S1 (Supporting Information). Both (*Z*)-*o*-BCaPTPE and (*Z*)-*o*-BTPATPE adopt a chiasmatic conformation, where intramolecular π–π stackings with distances of 3.274 and 3.417 Å are formed between phenyl rings. However, when 4-arylbenzophenones were used as starting materials, only mixtures of *Z*- and *E*-isomers were obtained. Although the detailed mechanism for the formation of sole *Z*-products from 2-arylbenzophenones is still under investigation, it is believed that the intramolecular π–π interaction should account for the stereoselectivity of the reactions. Such interaction helps rigidify and stabilize the intermediate complex of titanium species, whose subsequent deoxygenation furnishes the *Z*-products (**Scheme 2**).[7]

The rigid chiasmatic conformations of (*Z*)-*o*-BCaPTPE and (*Z*)-*o*-BTPATPE may strongly suppress the IMR process, which may endow the luminogens with high PL efficiencies in both

---

Dr. Z. Zhao, Prof. H. Qiu
College of Material
Chemistry and Chemical Engineering
Hangzhou Normal University
Hangzhou 310036, China
Dr. J. W. Y. Lam, C. Y. K. Chan, Dr. J. Liu, Dr. H. H. Y. Sung,
Prof. I. D. Williams, Prof. B. Z. Tang
Department of Chemistry
The Hong Kong University of Science & Technology (HKUST)
Clear Water Bay, Kowloon, Hong Kong, China
E-mail: tangbenz@ust.hk
S. Chen, Prof. H. S. Kwok
Center for Display Research
HKUST, Clear Water Bay, Kowloon, Hong Kong, China
Dr. P. Lu, Prof. Y. Ma
State Key Laboratory of Supramolecular Structure and Materials
Jilin University
Changchun 130012, China
Dr. M. Rodriguez, Dr. J.-L. Maldonado, Prof. G. Ramos-Ortiz
Centro de Investigaciones en Óptica
A. P. 1-948, 37000 León, Gto., México
Dr. H. Su, Prof. K. S. Wong
Department of Physics
HKUST, Clear Water Bay, Kowloon, Hong Kong, China

DOI: 10.1002/adma.201102804

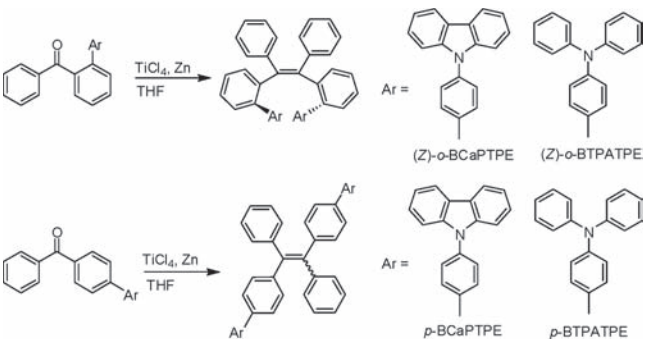

Scheme 1. Synthesis of TPE derivatives with chiasmatic and linear structures by McMurry reaction.

solution and aggregate states. This is indeed the case. (*Z*)-*o*-BCaPTPE and (*Z*)-*o*-BTPATPE show intense emissions at 497 and 510 nm with fluorescence quantum yields (Φ_F's) of 43 and 38%, respectively, in dilute tetrahydrofuran (THF) solutions (10 µM) (**Table 1**). The PL emissions of solid thin films of (*Z*)-*o*-BCaPTPE and (*Z*)-*o*-BTPATPE are observed at 477 and

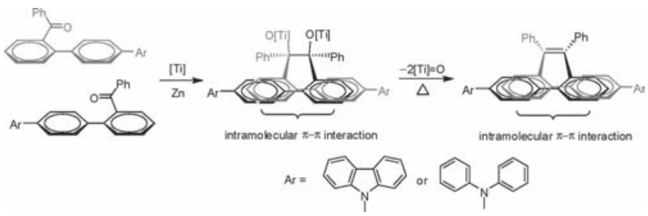

Scheme 2. Proposed mechanism for the formation of (*Z*)-*o*-BCaPTPE and (*Z*)-*o*-BTPATPE.

490 nm, respectively, while their crystals emit at shorter wavelengths of ≈456 nm (Figure S4, Supporting Information). A similar phenomenon was also observed in other TPE derivatives.[3,8,9] In the crystal state, the molecules of (*Z*)-*o*-BCaPTPE and (*Z*)-*o*-BTPATPE may have conformationally adjusted themselves by twisting their phenyl rings in order to fit into the crystalline lattices, thus leading to hypsochromic shift in their PL spectra. The absolute Φ_F's of (*Z*)-*o*-BCaPTPE and (*Z*)-*o*-BTPATPE films measured using an integrating sphere are as high as 100 and 85%, respectively. Such values are more than two-fold higher

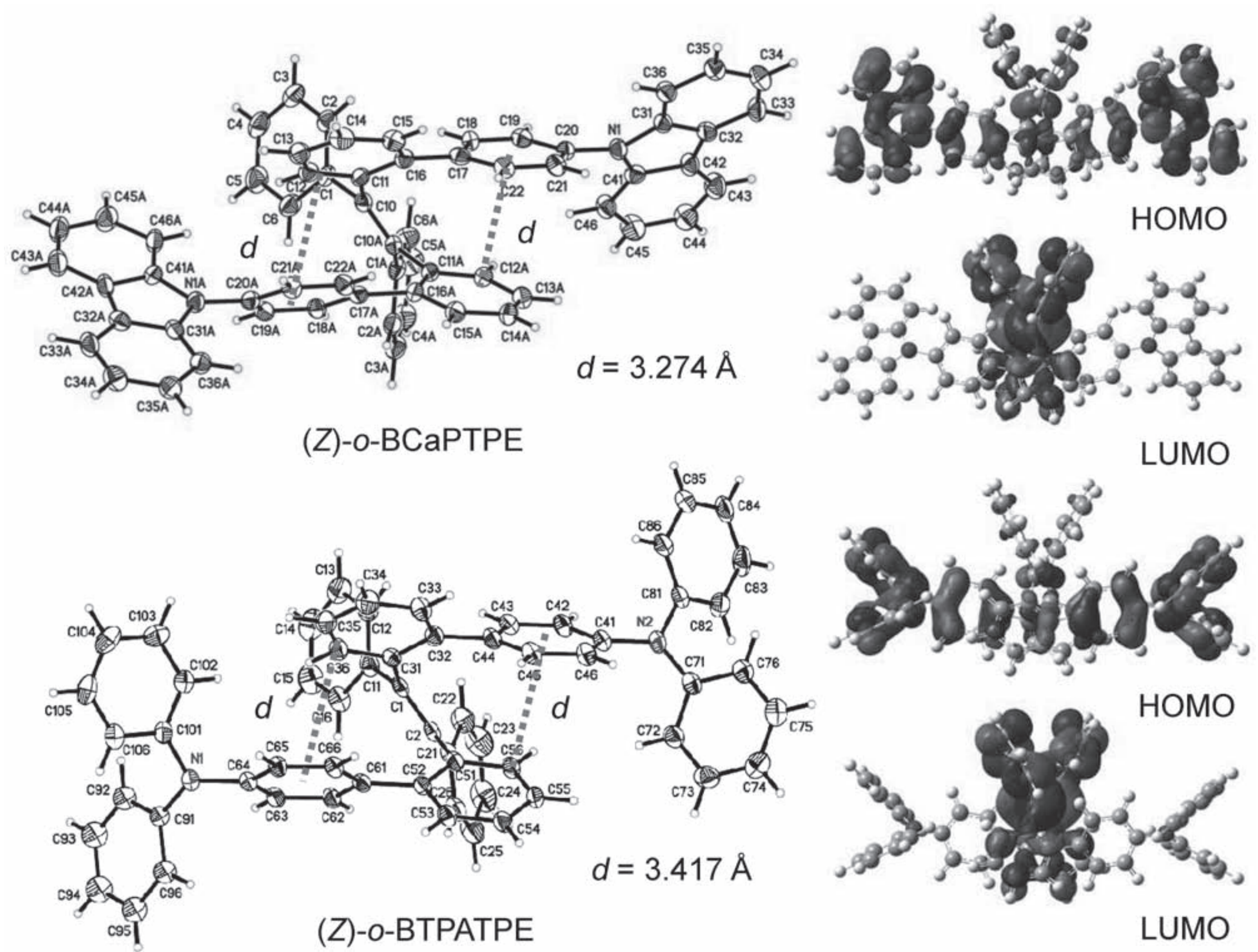

Figure 1. ORTEP drawings of (*Z*)-*o*-BCaPTPE (CCDC 825621) and (*Z*)-*o*-BTPATPE (CCDC 825622) and molecular orbital amplitude plots of their highest occupied molecular orbital (HOMO) and lowest unoccupied molecular orbital (LUMO) levels calculated at the B3LYP/6-31G(d) level.

Table 1. Optical and thermal properties, fluorescence lifetimes, and energy levels of the luminogens. Abbreviations: Soln = solution (10 μM in THF), Cryst = crystals, λ_{em} = PL maximum, α_{AIE} = extent of emission enhancement ($\Phi_{\text{Film}}/\Phi_{\text{Soln}}$), τ = fluorescence decay time measured in THF solution; excitation wavelength: 350 nm. Φ_{F} = absolute fluorescence quantum yield measured using an integrating sphere, T_{g} = glass transition temperature, T_{d} = onset decomposition temperature, HOMO and LUMO are estimated from theoretical calculations, E_{opt} = energy bandgap determined from the onset of absorption spectra.

	λ_{em} [nm]			Φ_{F} [%]			τ	$T_{\text{g}}/T_{\text{d}}$	HOMO/LUMO	E_{opt}
	Soln	Cryst	Film	Soln	Film	α_{AIE}	[ns]	[°C]	[eV]	[eV]
(*Z*)-*o*-BCaPTPE	497	456	477	43	100	2.3	4.7	222/427	−5.25/−1.44	3.33
(*Z*)-*o*-BTPATPE	510	457	490	38	85	2.2	2.7	127/421	−4.85/−1.18	3.20
p-BCaPTPE	498		487	0.5	100	200	0.061	221/491		3.07
p-BTPATPE[a)]	512		509	1.8	100	55	0.062	126/455		2.90

[a)] From ref. [15].

than those in solutions (the AIE effect α_{AIE} [1d,8a], a ratio of Φ_{F} in film to that in solution, is 2.3 for (*Z*)-*o*- BCaPTPE, and is 2.2 for (*Z*)-*o*- BTPATPE), demonstrating a feature of aggregation-enhanced emission (AEE). However, their linear counterparts show distinct emission behaviors. *p*-BCaPTPE and *p*-BTPATPE exhibit negligible emissions in solutions with Φ_{F}'s of merely 0.5 and 1.8%, respectively. Their solid films, however, emit intensely with unity efficiencies, leading to much higher α_{AIE} values (Table 1).

Fluorescence lifetime is an important kinetic parameter for the excited-state decay process and is closely associated with the fluorescence efficiency. Generally, the shorter the lifetime is, the lower the Φ_{F} value is.[10] To gain insight into the emission properties of the luminogens, we studied their dynamic behaviors in THF solutions (10 μM) using time-resolved fluorescence spectroscopy. Whereas the singlet excited states of *p*-BCaPTPE and *p*-BTPATPE decay rapidly with lifetimes as short as ≈60 ps at room temperature, (*Z*)-*o*-BCaPTPE and (*Z*)-*o*-BTPATPE show much higher values of 4.7 and 2.7 ns, respectively (Figure S5, Supporting Information). Clearly, the active IMR process of the TPE unit in *p*-BCaPTPE and *p*-BTPATPE has effectively consumed the excited state energy, thus rendering the luminogens weakly fluorescent in solutions. Thanks to the rigid chiasmatic conformation, the IMR process is partially hampered in (*Z*)-*o*-BCaPTPE and (*Z*)-*o*-BTPATPE. As a result, much stronger emissions are observed in their solutions.[2a,10b]

To further confirm the AEE feature of (*Z*)-*o*-BCaPTPE and (*Z*)-*o*-BTPATPE, we added water, a nonsolvent for both molecules, into their THF solutions and measured the PL change. As shown in **Figure 2**a, the emission of (*Z*)-*o*-BCaPTPE is increased gradually when the water fraction (f_{w}) in the solvent mixture becomes higher. Due to its immiscibility with the hydrophilic medium, the (*Z*)-*o*-BCaPTPE molecules must have been aggregated in aquesous mixtures with high water fractions. This restricts further the IMR process and hence enhances the light emission. Evidently, (*Z*)-*o*-BCaPTPE is a luminogen that exhibits AEE characteristic. It is noteworthy that the emission of (*Z*)-*o*-BCaPTPE is blue-shifted in aqueous mixtures with high f_{w}'s due to the morphological change in the aggregates from amorphous to crystalline, as revealed by the transmission electron microscopy (TEM) images and electron diffraction (ED) patterns at f_{w}'s of 70 and 99.5% (Figure S6, Supporting Information).

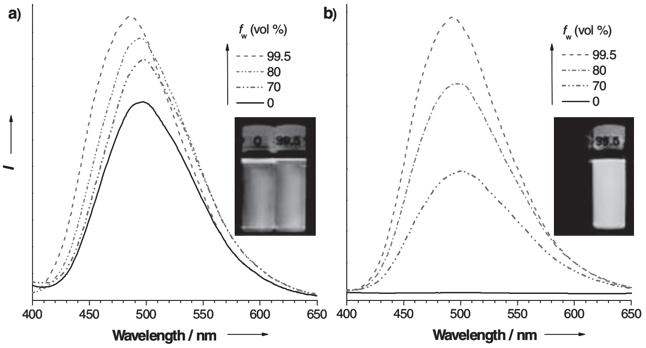

Figure 2. PL spectra of a) (*Z*)-*o*-BCaPTPE and b) *p*-BCaPTPE in THF/water mixtures with different f_{w}. Excitation wavelength: 350 nm.

(*Z*)-*o*-BTPATPE also shows similar emission behavior (Figure S7a, Supporting Information). On the other hand, the PL spectra of *p*-BCaPTPE and *p*-BTPATPE in THF are almost flat lines parallel to the abscissa. Intense signals, however, are recorded when they are aggregated in THF/water mixtures (Figure 2b and Figure S7b, Supporting Information).

In an effort to understand the mechanism for this AEE system, we checked the geometric structures and the packing arrangements of (*Z*)-*o*-BCaPTPE in the crystal state. Besides intramolecular π–π interactions as discussed above, multiple C–H$\cdots\pi$ hydrogen bonds with distances of 2.986 and 2.989 Å are formed between the phenyl proton of one molecule and the π cloud of the carbazole unit of adjacent molecule. **Figure 3** illustrates parts of C–H$\cdots\pi$ hydrogen bonds formed in (*Z*)-*o*-BCaPTPE crystals as an example. These multiple C–H$\cdots\pi$ hydrogen bonds plus the π–π interactions help rigidify the molecular conformation.[8c,d] The rotation of the phenyl rings attached to the central vinyl stator is locked by such bonding in the crystal state. As a result, the excited state energy consumed by the IMR process is greatly reduced, making the luminogens stronger emitters in the solid state.

We carried out theoretical calculations of (*Z*)-*o*-BCaPTPE and (*Z*)-*o*-BTPATPE in order to understand their photophysical properties at the molecular level. The density functional theory with B3LYP hybrid functional at the basis set level of 6-31G(d) was used for the calculation. As shown in Figure 1, the HOMOs

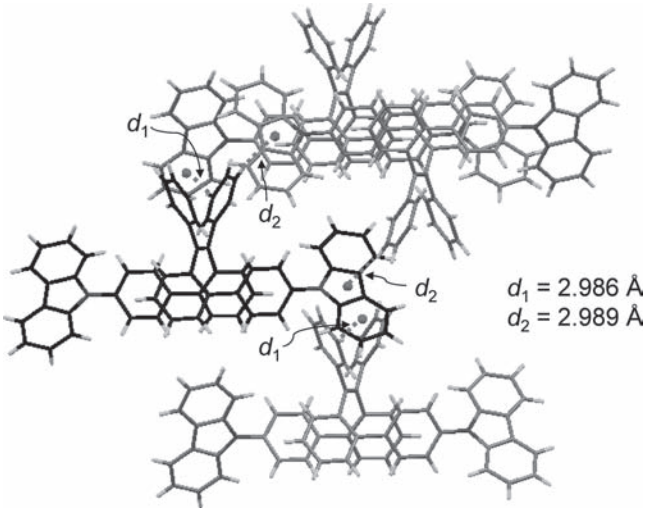

Figure 3. C–H···π hydrogen bonds formed between adjacent molecules of (*Z*)-*o*-BCaPTPE in the crystal state. For clarity, only parts of C–H···π hydrogen bonds are indicated as examples.

of both luminogens are dominated by the orbitals from the carbazole or triphenylamine units. In contrast, the electron clouds of the LUMOs are mainly located on the TPE unit. Thus, increasing the stiffness of the TPE conformation will hamper the nonradiative decay of the excitons as they are more likely to be confined in the central core during the PL process.[11] (*Z*)-*o*-BTPATPE has higher HOMO and LUMO energy levels than (*Z*)-*o*-BCaPTPE (Table 1). Both of them possess shorter effective conjugation lengths than their linear counterparts,[12] as revealed by their blue-shifted absorption spectra (Figure S8, Supporting Information) and wider energy bandgaps.

Both (*Z*)-*o*-BCaPTPE and (*Z*)-*o*-BTPATPE are thermally stable. As shown in Figure S9 (Supporting Information), they start to decompose at temperatures (T_d) as high as 427 and 421 °C. The glass transition temperatures (T_g) are detected at 222 and 127 °C for (*Z*)-*o*-BCaPTPE and (*Z*)-*o*-BTPATPE, respectively, revealing that they also enjoy high morphological stability. The data are close to those of their linear counterparts, suggesting that all the luminogens share similar thermal properties, irrespective of their conformations (Table 1). The T_d and T_g of (*Z*)-*o*-BCaPTPE are higher than those of (*Z*)-*o*-BTPATPE, probably due to the higher rigidity of the carbazole unit.

In contrast to many organic materials, where the charge transport is dominated by either holes or electrons, the chiasmatic conformation of (*Z*)-*o*-BCaPTPE and (*Z*)-*o*-BTPATPE has endowed them with interesting bipolar charge transport capability. We used time-of-flight (TOF) transient photocurrent technique to investigate their charge mobility. (*Z*)-*o*-BCaPTPE- or (*Z*)-*o*-BTPATPE-doped poly(styrene) (PS) films (10 μm) with or without C_{60} were prepared and sandwiched between two indium tin oxide (ITO)-coated glass slides for the measurement. The efficient PL emissions of (*Z*)-*o*-BCaPTPE and (*Z*)-*o*-BTPATPE in the solid state suggest that the probability for exciton generation is very high in their photophysical process. Thus, the introduction of C_{60} to the PS film is to facilitate the exciton dissociation and hence increases the efficiency for charge carrier generation owing to its strong electron-accepting capability.[13] The (*Z*)-*o*-BCaPTPE:PS:C_{60} composite exhibits a higher photocurrent, which gives a better plot from which the charge mobility can be measured. The photogeneration and charge transport are confirmed by the follows: i) Dark current is found to be negligible under the bias configuration. In this case, under photoexcitation but with zero external electric field, no photocurrent is detected. ii) When an external electric field is applied to the sample in the absence of photoexcitation, no charge transport occurrs. In contrast, photocurrents are readily detected when a biased sample is photoexcited. **Figure 4** shows the transient photocurrents of (*Z*)-*o*-BCaPTPE:PS:C_{60} (50:48.5:1.5 wt%) film at applied fields of 40 and 60 V μm^{-1} as an example. The detected photocurrent is dispersive. Since the charge transportation in films fabricated from organic materials occurs via a hopping process, the dispersive behavior can be explained by the presence of traps such as oxygen and water that may arise during the film preparation.[14]

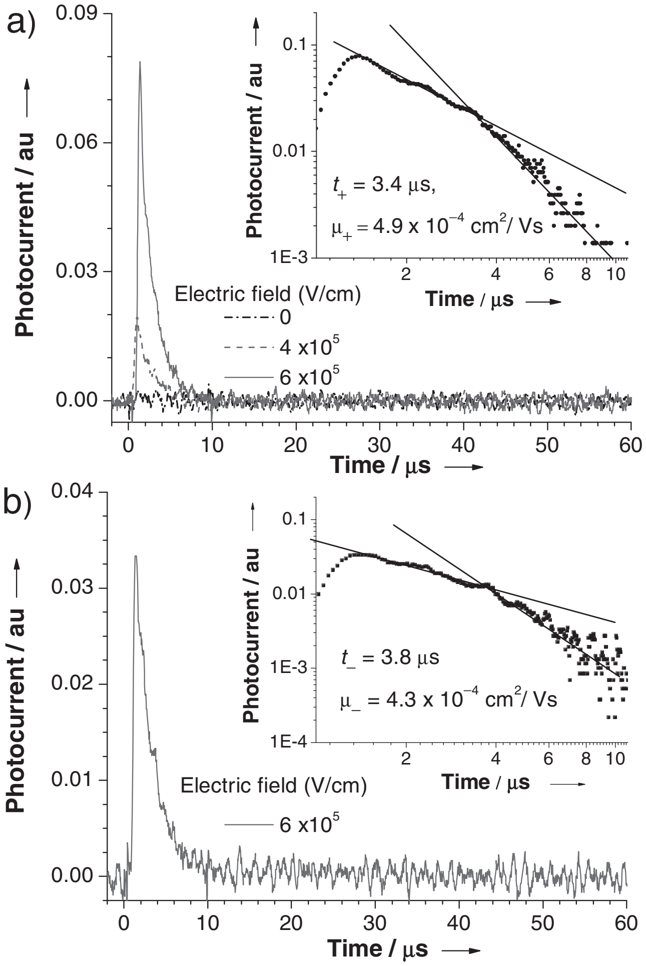

Figure 4. Transient photocurrents in a) hole transport and b) electron transport configurations for film (10 μm) of (*Z*)-*o*-BCaPTPE:PS:C_{60} (50:48.5:1.5 wt%) composite. Inset: log–log plot of the photocurrent as a function of time.

As shown in Figure 4a, the transient photocurrents for holes increase as the bias voltage becomes higher. The transient time determined from the logarithmic plot is 3.4 μs at an applied electric field of 60 V μm^{-1}, from which a hole mobility of 4.9×10^{-4} cm^2 V^{-1} s^{-1} is determined. This value is approximately five-fold higher than that of *N*,*N*′-diphenyl-*N*,*N*′-bis(3-methylphenyl)-1,1′-biphenyl-4,4′-diamine (TPD) under the same measurement conditions.[13a]

Interestingly, photocurrent for electrons was also detected when the polarity of the applied bias was switched (Figure 4b). The transient time determined from the logarithmic plot is 3.8 μs at 60 V μm^{-1}, corresponding to an electron mobility of 4.3×10^{-4} cm^2 V^{-1} s^{-1} for (*Z*)-*o*-BCaPTPE. This value is close to that of hole mobility and is more than one-order higher than that of tris(8-hydroxyquinolinolato)aluminium (Alq$_3$), a widely used electron-transporting material.[14b] (*Z*)-*o*-BTPATPE also shows similar bipolar charge transport property (Figure S10, Supporting Information) and its hole and electron mobilities are 3.7×10^{-4} and 3.3×10^{-4} cm^2 V^{-1} s^{-1}, respectively. Since *p*-BTPATPE shows a hole mobility of 5.2×10^{-4} cm^2 V^{-1} s^{-1}[15] but exhibits no electron transport property, this suggests that the chiasmatic conformation of (*Z*)-*o*-BCaPTPE and (*Z*)-*o*-BTPATPE plays a key role for the high electron mobility of the molecules. (*Z*)-*o*-BCaPTPE exhibits higher hole and electron mobilities than (*Z*)-*o*-BTPATPE, presumably due to its more rigid conformation and stronger intramolecular π–π interaction.

The efficient solid-state PL efficiency and bipolar charge mobility of (*Z*)-*o*-BCaPTPE and (*Z*)-*o*-BTPATPE inspire us to explore their multifunctionality in optoelectronic devices. We fabricated three kinds of organic light-emitting diodes (OLEDs) with configurations of a) ITO/(*Z*)-*o*-BCaPTPE or (*Z*)-*o*-BTPATPE (80 nm)/TPBi (10 nm)/Alq$_3$ (30 nm)/LiF (1 nm)/Al (100 nm), in which (*Z*)-*o*-BCaPTPE and (*Z*)-*o*-BTPATPE serve as both hole-transporting and light-emitting layers and 1,3,5-tris(*N*-phenylbenzimidazol-2-yl)benzene (TPBi) and Alq$_3$ function as hole-blocking and electron-transporting layers, respectively; b) ITO/NPB (60 nm)/(*Z*)-*o*-BCaPTPE or (*Z*)-*o*-BTPATPE (60 nm)/LiF (1 nm)/Al (100 nm), in which (*Z*)-*o*-BCaPTPE and (*Z*)-*o*-BTPATPE serve as both light-emitting and electron-transporting layers and *N*,*N*′-di(1-naphthyl)-*N*,*N*′-diphenyl-benzidine (NPB) acts as hole-transporting layer; and c) ITO/NPB (60 nm)/(*Z*)-*o*-BCaPTPE or (*Z*)-*o*-BTPATPE (20 nm)/TPBi (10 nm)/Alq$_3$ (30 nm)/LiF (1 nm)/Al (100 nm), in which (*Z*)-*o*-BCaPTPE and (*Z*)-*o*-BTPATPE serve as light-emitting layers only. The performance data of the devices are summarized in **Table 2** and the characteristic curves are given in Figure S11,S12 (Supporting Information). Both luminogens show sky blue EL at 488–492 nm. The EL spectra are similar to the PL spectra of their films and change little with the applied voltage, indicating that the EL originates from the same radiative decay of the singlet excitons. The maximum current efficiencies attained by the devices are observed at low current densities and decay quicky with increasing current density. This is in some sense understandable because the device structures are not yet optimized. Exciton leakage to NPB or TPBi layers and quenching under high electric filed, accumulation of holes, etc., may cause the efficiency drops quickly at high current density.

Because of the high bipolar charge mobility, the EL devices of the chiasmatic luminogens without NPB or TPBi/Alq$_3$ layers perform well and show good EL efficiency. Device (a) of (*Z*)-*o*-BCaPTPE without NPB shows a maximum current efficiency ($\eta_{C,max}$) of 4.8 cd A^{-1} and an external quantum efficiency ($\eta_{ext,max}$) of 2.1%. Much better performances are observed in device (b) fabricated in the absence of TPBi/Alq$_3$ layers. The $\eta_{C,max}$ and $\eta_{ext,max}$ reach 7.9 cd A^{-1} and 3.1%, respectively, which are even higher than those of device (c) that contains both NPB and TPBi/Alq$_3$ layers. These results prove again that (*Z*)-*o*-BCaPTPE possesses outstanding hole- and electron-transporting capabilities in addition to excellent light-emitting properties. (*Z*)-*o*-BTPATPE can also serve as a multifunctional material in OLEDs but its EL performances are inferior to those of (*Z*)-*o*-BCaPTPE due to its comparatively lower solid-state PL efficiency and bipolar charge mobility. Unlike (*Z*)-*o*-BCaPTPE, the device (a) of (*Z*)-*o*-BTPATPE shows a lower turn-on voltage and higher efficiencies than those of devices (b) and (c) (Table 2). This suggests that (*Z*)-*o*-BTPATPE is in favor of hole injection, while (*Z*)-*o*-BCaPTPE prefers electron injection due to its relatively lower HOMO energy level.

Table 2. EL performances of (*Z*)-*o*-BCaPTPE and (*Z*)-*o*-BTPATPE. Device configuration: a) ITO/(*Z*)-*o*-BCaPTPE or (*Z*)-*o*-BTPATPE (80 nm)/TPBi (10 nm)/Alq$_3$ (30 nm)/LiF (1 nm)/Al (100 nm), b) ITO/NPB (60 nm)/(*Z*)-*o*-BCaPTPE or (*Z*)-*o*-BTPATPE (60 nm)/LiF (1 nm)/Al (100 nm), and c) ITO/NPB (60 nm)/(*Z*)-*o*-BCaPTPE or (*Z*)-*o*-BTPATPE (20 nm)/TPBi (10 nm)/Alq$_3$ (30 nm)/LiF (1 nm)/Al (100 nm). Abbreviations: λ_{EL} = EL maximum, V_{on} = turn-on voltage at 1 cd m^{-2}, L_{max} = maximum luminance, $\eta_{C,max}$ = maximum current efficiency, and $\eta_{ext,max}$ = maximum external quantum efficiency.

active layer	λ_{EL} [nm]	V_{on} [V]	L_{max} [cd m^{-2}]	$\eta_{C,max}$ [cd A^{-1}]	$\eta_{ext,max}$ [%]
a) (*Z*)-*o*-BCaPTPE	489	6.8	6250	4.8[a)]	2.1
b) (*Z*)-*o*-BCaPTPE	492	4.5	8010	7.9[b)]	3.1
c) (*Z*)-*o*-BCaPTPE	488	6.8	5890	5.8[c)]	2.6
a) (*Z*)-*o*-BTPATPE	488	3.4	7070	5.1[d)]	2.4
b) (*Z*)-*o*-BTPATPE	492	8.0	9060	3.3[e)]	1.3
c) (*Z*)-*o*-BTPATPE	492	4.3	6420	4.7[f)]	2.0

[a)] At 30 cd m^{-2}; [b)] At 100 cd m^{-2}; [c)] At 60 cd m^{-2}; [d)] At 50 cd m^{-2}; [e)] At 80 cd m^{-2}; [f)] At 28 cd m^{-2}.

For comparison, control OLEDs with configurations of a) ITO/*p*-BCaPTPE or *p*-BTPATPE (80 nm)/TPBi (10 nm)/Alq$_3$ (30 nm)/LiF (1 nm)/Al (100 nm) and b) ITO/NPB (60 nm)/*p*-BCaPTPE or *p*-BTPATPE (60 nm)/LiF (1 nm)/Al (100 nm) were fabricated, in which the linear luminogens take the same roles as those of chiasmatic luminogens mentioned above. Their performance curves are given in Figure S13 (Supporting Information). *p*-BCaPTPE and *p*-BTPATPE function well as both hole-transporting and light-emitting layers in device (a). However, the performances of device (b) based on both luminogens are very poor, revealing that *p*-BCaPTPE and *p*-BTPATPE are not promising electron-transporting materials. These results further evidence that the high electron mobilities of (*Z*)-*o*-BCaPTPE and (*Z*)-*o*-BTPATPE stem from their novel chiasmatic conformations.

In summary, stereoregular TPE derivatives (*Z*)-*o*-BCaPTPE and (*Z*)-*o*-BTPATPE were first synthesized by McMurry reaction in moderate yields. Although most TPE derivatives with linear structures such as *p*-BCaPTPE and *p*-BTPATPE are weakly fluorescent in solutions, (*Z*)-*o*-BCaPTPE and (*Z*)-*o*-BTPATPE, with their chiasmatic conformations, can emit intensely in the solution state due to the intramolecular π–π interactions, which restricts the IMR process and hence promotes radiative decay of the excitons. (*Z*)-*o*-BCaPTPE and (*Z*)-*o*-BTPATPE emit as efficient as their linear counterparts in the solid state and enjoy similarly high morphologically and thermally stabilities. Their chiasmatic conformation coupled with intramolecular π–π stacking endows them with fascinating material properties. *p*-BCaPTPE and *p*-BTPATPE with linear structures exhibit hole-transporting property only, but (*Z*)-*o*-BCaPTPE and (*Z*)-*o*-BTPATPE show bipolar charge mobility, although they are constructed from hole-transporting building blocks. High hole and electron mobilities up to 4.9×10^{-4} and 4.3×10^{-4} cm^2 V^{-1} s^{-1}, respectively, have been detected in (*Z*)-*o*-BCaPTPE. The chiasmatic luminogens can serve as multifunctional materials in OLEDs. The device fabricated using (*Z*)-*o*-BCaPTPE as both the light-emitting and electron-transporting layers exhibits high efficiencies up to 7.9 cd A^{-1} and 3.1%, although the device structure is not yet optimized. Such attributes make the chiasmatic luminogens a new type of promising materials for optoelectronic devices.

Supporting Information

Supporting Information is available from the Wiley Online Library or from the author.

Acknowledgements

The authors thank Dr. Chunmei Deng and Prof. Zhigang Shuai for theoretical calculation. This project was partially supported by the Research Project Competition of HKUST (RPC11SC09), Research Grants Council of Hong Kong (604711, 603509, and HKUST2/CRF/10), the University Grants Committee of Hong Kong (AoE/P-03/08). Z.J.Z. acknowledges the financial support from Natural Science Foundation of Zhejiang Province (Y4110331). J.-L.M. and G.R.-O. acknowledge grants from CONACYT (55250 and J-49512).

Received: July 21, 2011
Revised: August 27, 2011

---

[1] a) J. Luo, Z. Xie, J. W. Y. Lam, L. Cheng, H. Chen, C. Qiu, H. S. Kwok, X. Zhan, Y. Liu, D. Zhu, B. Z. Tang, *Chem. Commun.* **2001**, 1740; b) Z. Zhao, Z. Wang, P. Lu, C. Y. K. Chan, D. Liu, J. W. Y. Lam, H. H. Y. Sung, I. D. Williams, Y. Ma, B. Z. Tang, *Angew. Chem. Int. Ed.* **2009**, *48*, 7608; c) Y. Hong, J. W. Y. Lam, B. Z. Tang, *Chem. Commun.* **2009**, 4332; d) Y. Hong, J. W. Lam, B. Z. Tang, *Chem. Soc. Rev.* **2011**, DOI: 10.1039/c1cs15113d.
[2] a) Z. Li, Y. Dong, B. Mi, Y. Tang, M. Häußler, H. Tong, Y. Dong, J. W. Y. Lam, Y. Ren, H. H. Y. Sun, K. S. Wong, P. Gao, I. D. Williams, H. S. Kwok, B. Z. Tang, *J. Phys. Chem. B* **2005**, *109*, 10061; b) S. Dong, Z. Li, J. Qin, *J. Phys. Chem. B* **2009**, *113*, 434; c) G. Yu, S. Yin, Y. Liu, J. Chen, X. Xu, X. Sun, D. Ma, X. Zhan, Q. Peng, Z. Shuai, B. Z. Tang, D. Zhu, W. Fang, Y. Luo, *J. Am. Chem. Soc.* **2005**, *127*, 6335.
[3] a) Y. Liu, C. Deng, L. Tang, A. Qin, R. Hu, J. Z. Sun, B. Z. Tang, *J. Am. Chem. Soc.* **2011**, *133*, 660; b) Z. Zhao, J. W. Y. Lam, B. Z. Tang, *Curr. Org. Chem.* **2010**, *14*, 2109.
[4] V. S. Vyas, R. Rathore, *Chem. Commun.* **2010**, *46*, 1065.
[5] J. E. McMurry, M. P. Felming, *J. Am. Chem. Soc.* **1974**, *96*, 4708.
[6] a) R. Daik, W. J. Feast, A. S. Batsanov, J. A. K. Howard, *New J. Chem.* **1998**, 1047; b) X.-F. Duan, J. Zeng, J.-W. Lü, Z.-B. Zhang, *J. Org. Chem.* **2006**, *71*, 9873.
[7] a) M. Ephritikhine, *Chem. Commun.* **1998**, 2549; b) A. Fürstner, B. Bogdanović, *Angew. Chem. Int. Ed.* **1996**, *35*, 2442.
[8] a) Z. Zhao, S. Chen, X. Shen, F. Mahtab, Y. Yu, P. Lu, J. W. Y. Lam, H. S. Kwok, B. Z. Tang, *Chem. Commun.* **2010**, *46*, 686; b) Z. Zhao, S Chen, J. W. Y. Lam, P. Lu, Y. Zhong, K. Wong, H. S. Kwok, B. Z. Tang, *Chem. Commun.* **2010**, *46*, 2221; c) Z. Zhao, P. Lu, J. W. Y. Lam, Z. Wang, C. Y. K. Chan, H. H. Y. Sung, I. D. Williams, Y. Ma, B. Z. Tang, *Chem. Sci.* **2010**, *2*, 672; d) Z. Zhao, S. Chen, J. W. Y. Lam, Z. Wang, P. Lu, F. Mahtab, H. H. Y. Sung, I. D. Williams, Y. Ma, H. S. Kwok, B. Z. Tang, *J. Mater. Chem.* **2011**, *21*, 7210.
[9] a) M. Wang, G. Zhang, D. Zhang, D. Zhu, B. Z. Tang, *J. Mater. Chem.* **2010**, *20*, 1858; b) L. Liu, G. Zhang, J. Xiang, D. Zhang, D. Zhu, *Org. Lett.* **2008**, *10*, 4581.
[10] a) Y. Ren, J. W. Y. Lam, Y. Dong, B. Z. Tang, K. S. Wong, *J. Phys. Chem. B* **2005**, *109*, 1135; b) J. Liu, Y. Zhong, J. W. Y. Lam, P. Lu, Y. Hong, Y. Yu, Y. Yue, F. Mahtab, H. H. Y. Sung, I. D. Williams, K. S. Wong, B. Z. Tang, *Macromolecules* **2010**, *43*, 4921.
[11] a) R. Nandy, M. Subramoni, B. Varghese, S. Sankararaman, *J. Org. Chem.* **2007**, *72*, 938; b) S. Sankararaman, G. Venkataramana, B. Varghese, *J. Org. Chem.* **2008**, *73*, 2404; c) Z. Zhao, S. Chen, J. W. Y. Lam, Z. Wang, P. Lu, F. Mahtab, H. H. Y. Sung, I. D. Williams, Y. Ma, H. S. Kwok, B. Z. Tang, *J. Mater. Chem.* **2011**, *21*, 7210.
[12] Y. Liu, S. Chen, J. W. Y. Lam, P. Lu, R. T. K. Kwok, F. Mahtab, H. S. Kwok, B. Z. Tang, *Chem. Mater.* **2011**, *23*, 2536.
[13] a) J.-L. Maldonado, G. Ramos-Ortiz, M. A. Meneses-Nava, O. Barbosa-Garcia, M. Olmos-Lopez, E. Arias, I. Moggio, *Opt. Mater.* **2007**,*29*, 821; b) J. J. M. Halls, K. Pichler, R. H. Friend, S. C. Moratti, A. B. Holmes, *Appl. Phys. Lett.* **1996**, *68*, 3120.
[14] a) A. R. Inigo, C. H. Tan, W. Fann, Y.-S. Huang, G.-Y. Perng, S.-A. Chen, *Adv. Mater.* **2001**, *13*, 504; b) G. G. Malliaras, Y. Shen, D. H. Dunlap, H. Murata, Z. H. Kafafi, *Appl. Phys. Lett.* **2001**, *79*, 2582; c) S. Naka, H. Okada, H. Onnagawa, Y. Yamaguchi, T. Tsutsui, *Synth. Met.* **2000**, *111–112*, 331; d) S. V. Novikov, *Phys. Status Solidi* **2003**, *236*, 119.
[15] Z. Zhao, Z. Li, J. W. Y. Lam, J.-L. Maldonado, G. Ramos-Ortiz, Y. Liu, W. Yuan, J. Xu, Q. Miao, B. Z. Tang, *Chem. Commun.* **2011**, *47*, 6924.